Characterisation of a primordial SGWB

Power spectrum of the GW energy density $\frac{d\rho_{\rm GW}}{d\log k}$

$$\rho_{\rm GW} = \frac{\langle \dot{h}_{ij}(\mathbf{x},t)\, \dot{h}_{ij}(\mathbf{x},t)\rangle}{32\pi G} = \frac{\langle h'_{ij}(\mathbf{x},\eta)\, h'_{ij}(\mathbf{x},\eta)\rangle}{32\pi G\, a^2(\eta)} = \int_0^{+\infty} \frac{dk}{k}\, \frac{d\rho_{\rm GW}}{d\log k}$$

$$\langle h'_r(\mathbf{k},\eta)\, {h'_p}^*(\mathbf{q},\eta)\rangle = \frac{8\pi^5}{k^3}\, \delta^{(3)}(\mathbf{k}-\mathbf{q})\, \delta_{rp}\, {h'_c}^2(k,\eta)$$

For *freely propagating sub-Hubble modes*, and taking the time-average:

$${h'_c}^2(k,\eta) \simeq k^2\, h_c^2(k,\eta) \qquad\qquad \frac{d\rho_{\rm GW}}{d\log k} = \frac{k^2\, h_c^2(k,\eta)}{16\pi G\, a^2(\eta)}$$

$$\rho_{\rm GW} \propto \frac{1}{a(\eta)^4}$$

GW energy density scales like radiation for freely propagating sub-Hubble modes (free massless particles)

Characterisation of a primordial SGWB

GW energy density parameter

Evaluated today, for a source that operated at time η_*

$$h^2\,\Omega_{\rm GW}(k,\eta_0) = \frac{h^2\rho_*}{\rho_c}\left(\frac{a_*}{a_0}\right)^4\left(\frac{1}{\rho_*}\frac{d\rho_{\rm GW}}{d\log k}(k,\eta_*)\right)$$

To make connection with the <u>detection process</u> one assumes that

- The source has stopped operating so the waves are freely propagating
- The expansion of the universe is negligible over the time of the measurement so that the SGWB appears stationary
- One can F.T. in time as well $\quad f = \frac{1}{2\pi}\frac{k}{a_0}$

Power spectral density

$$\langle \bar{h}_r(f,\hat{\mathbf{k}})\bar{h}^*_p(g,\hat{\mathbf{q}})\rangle = a_0^4\, f^2\, g^2 \langle A_r(\mathbf{k})\, A^*_p(\mathbf{q})\rangle = \\ = \frac{1}{8\pi}\,\delta(f-g)\,\delta^{(2)}(\hat{\mathbf{k}}-\hat{\mathbf{q}})\,\delta_{rp}\,S_h(f)$$

$$\Omega_{\rm GW}(f) = \frac{4\pi^2}{3H_0^2}\, f^3\, S_h(f)$$

Characterisation of a primordial SGWB

characteristic frequency of the SGWB signal

$$\boxed{f_* = \frac{1}{\ell_*} \geq H_*}$$

$$\epsilon_* = \ell_* H_*$$

Ratio of the typical length-scale of the GW sourcing process (size of the anisotropic stresses) and the Hubble scale at the generation time

$$f = f_* \frac{a_*}{a_0} = \frac{1.65 \times 10^{-7}}{\epsilon_*} \left(\frac{g(T_*)}{100} \right)^{1/6} \frac{T_*}{\text{GeV}} \,\text{Hz}$$

Characteristic frequency of the GW signal

$\epsilon_* = 1$

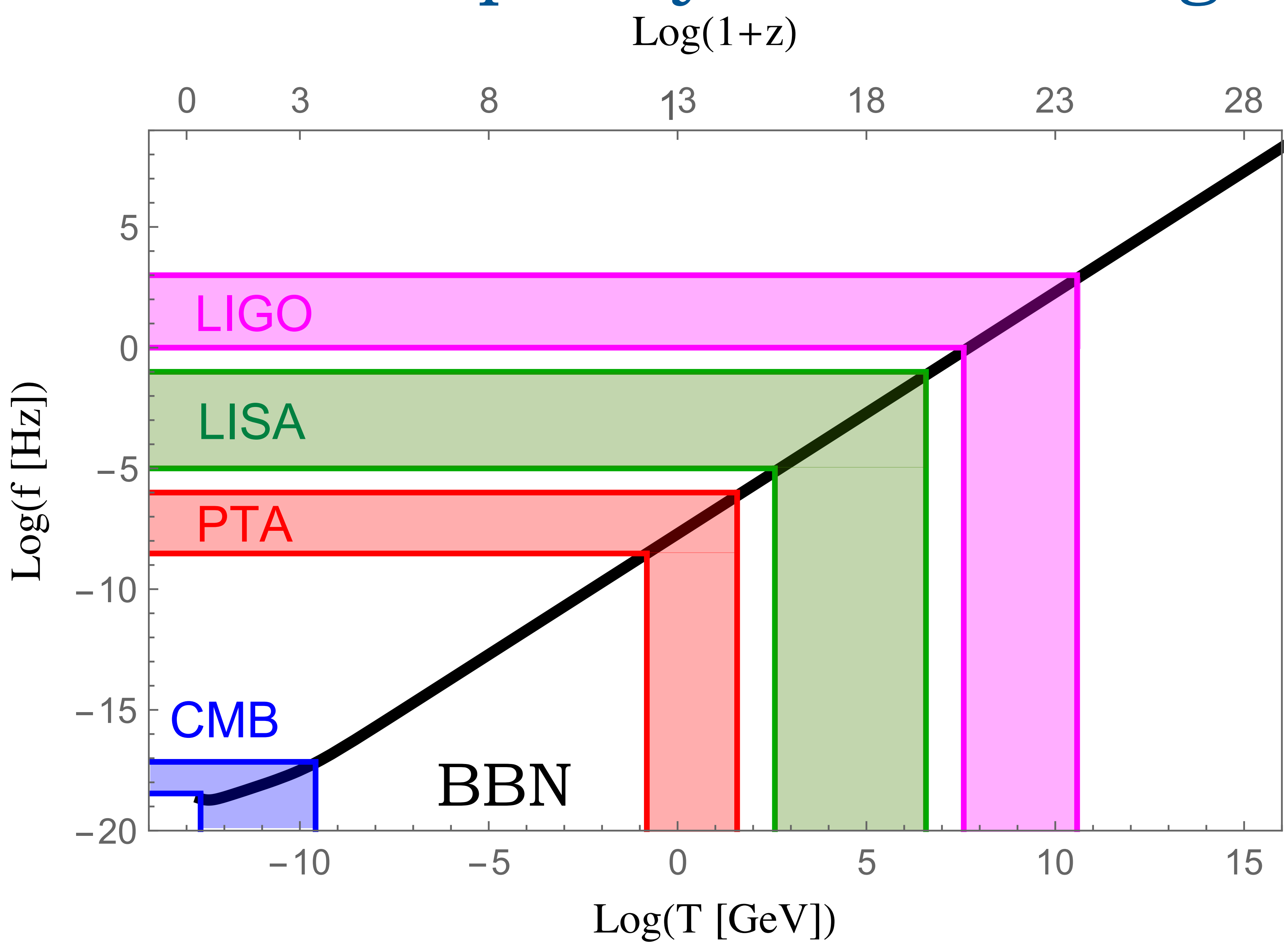

$T_{\rm QCD} \sim 100\,\mathrm{MeV}$	$\ell_* H_* \sim 1$	$\longrightarrow$	$f \sim 10\,\mathrm{nHz}$	PTA
$T_{\rm EW} \sim 100\,\mathrm{GeV}$	$\ell_* H_* \sim 0.01$	$\longrightarrow$	$f \sim \mathrm{mHz}$	LISA
$T_{\rm PQ} \sim 10^9\,\mathrm{GeV}$	$\ell_* H_* \sim 1$	$\longrightarrow$	$f \sim 100\,\mathrm{Hz}$	LVK

Discovery potential of primordial SGWB detection

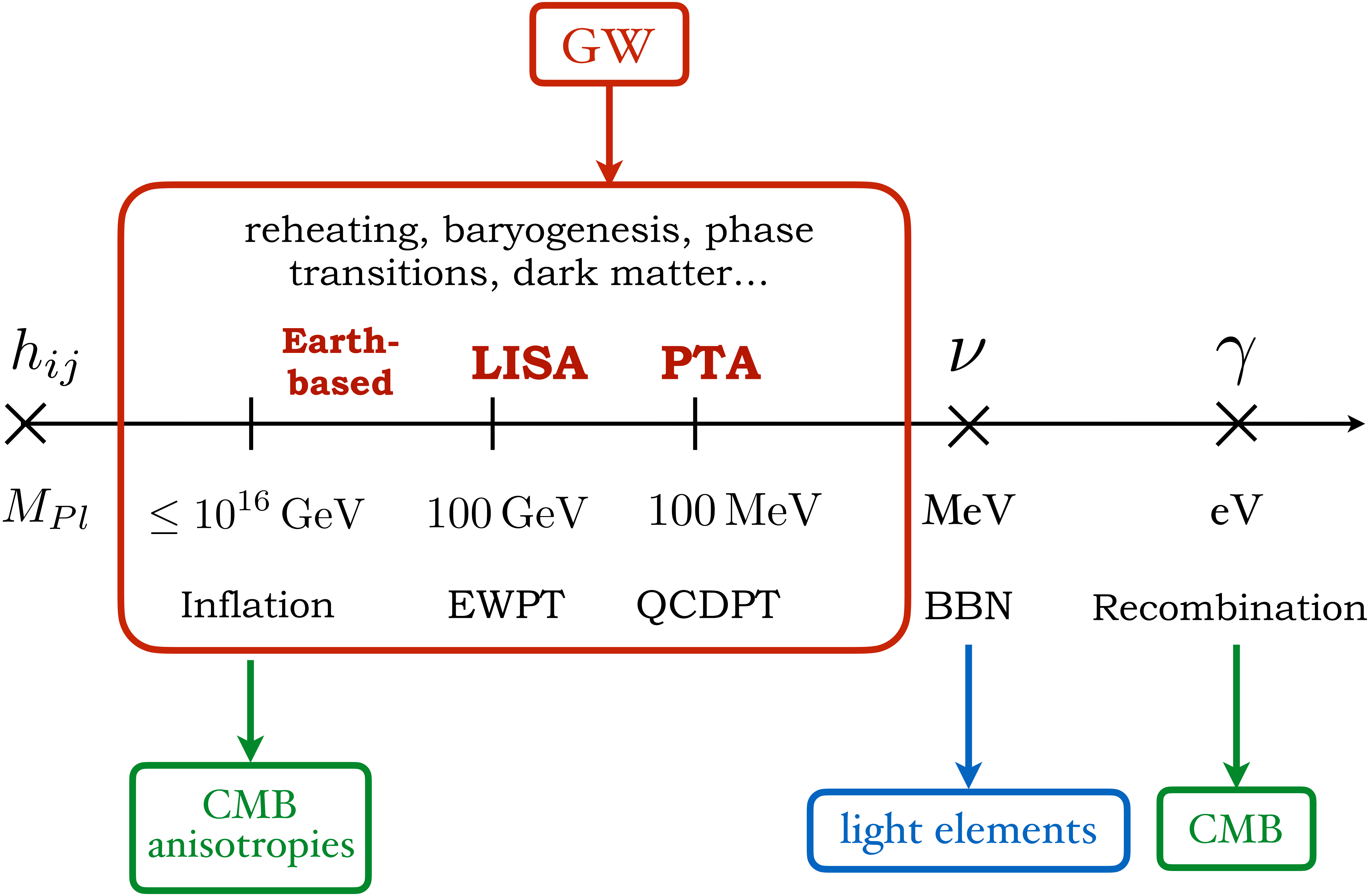

What is/will be known about the SGWB

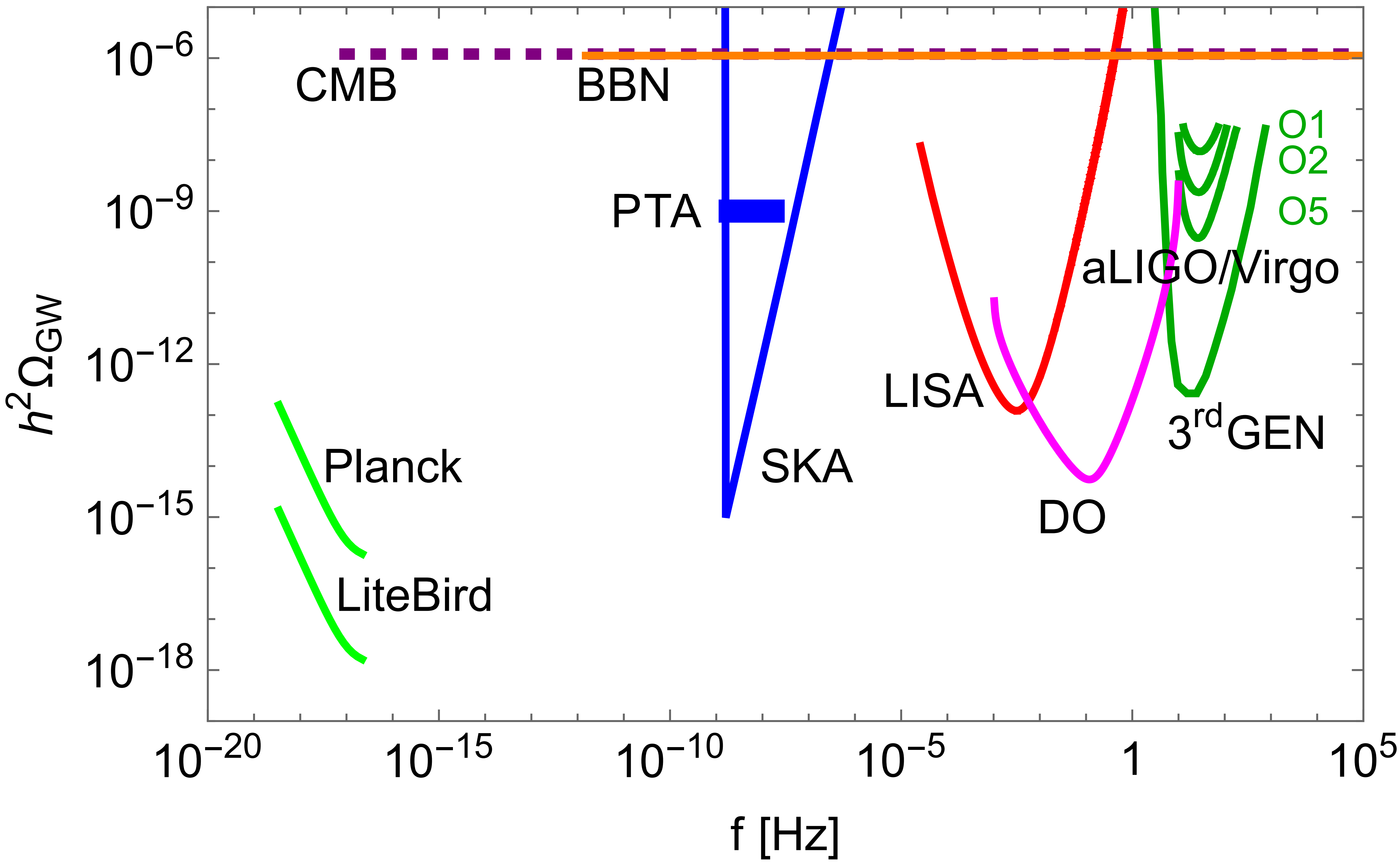

What is/will be known about the SGWB

Integrated upper bounds from radiation-like energy density

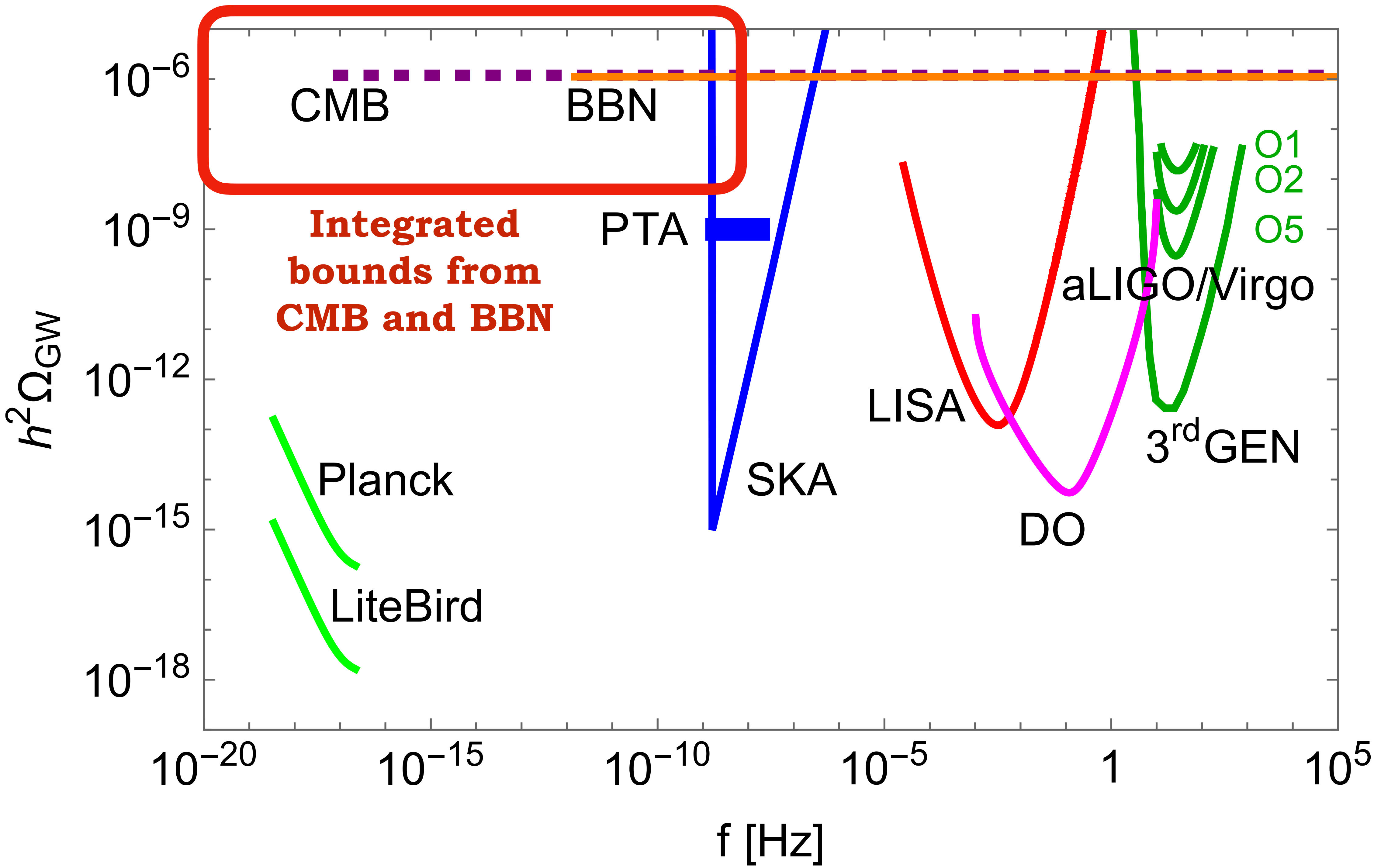

What is/will be known about the SGWB

- GW contribute to the energy density in the universe and change its background evolution

$$H^2(T) = \frac{8\pi G}{3} \Sigma_i \rho_i(T)$$

- The abundances of elements produced at Big Bang Nucleosynthesis (BBN) depend on the relative abundance of neutrons and protons, which depends on the Hubble scale at T ~ MeV

- The Cosmic Microwave Background (CMB) monopole and anisotropy spectrum depend on the Hubble scale at decoupling T ~ 0.3 eV, on the matter-radiation equality…

- Bounds on the *integrated GW energy density* at/previous to the BBN and CMB epochs

$$\left(\frac{\rho_{\rm GW}}{\rho_c}\right)_0 = \int \frac{df}{f}\,\Omega_{\rm GW}(f) = \Omega_\gamma^0 \left(\frac{g_S(T_0)}{g_S(T)}\right)^{4/3} \boxed{\left(\frac{\rho_{\rm GW}}{\rho_\gamma}\right)_T}$$

CAREFUL! Plot “wrong”…

What is/will be known about the SGWB

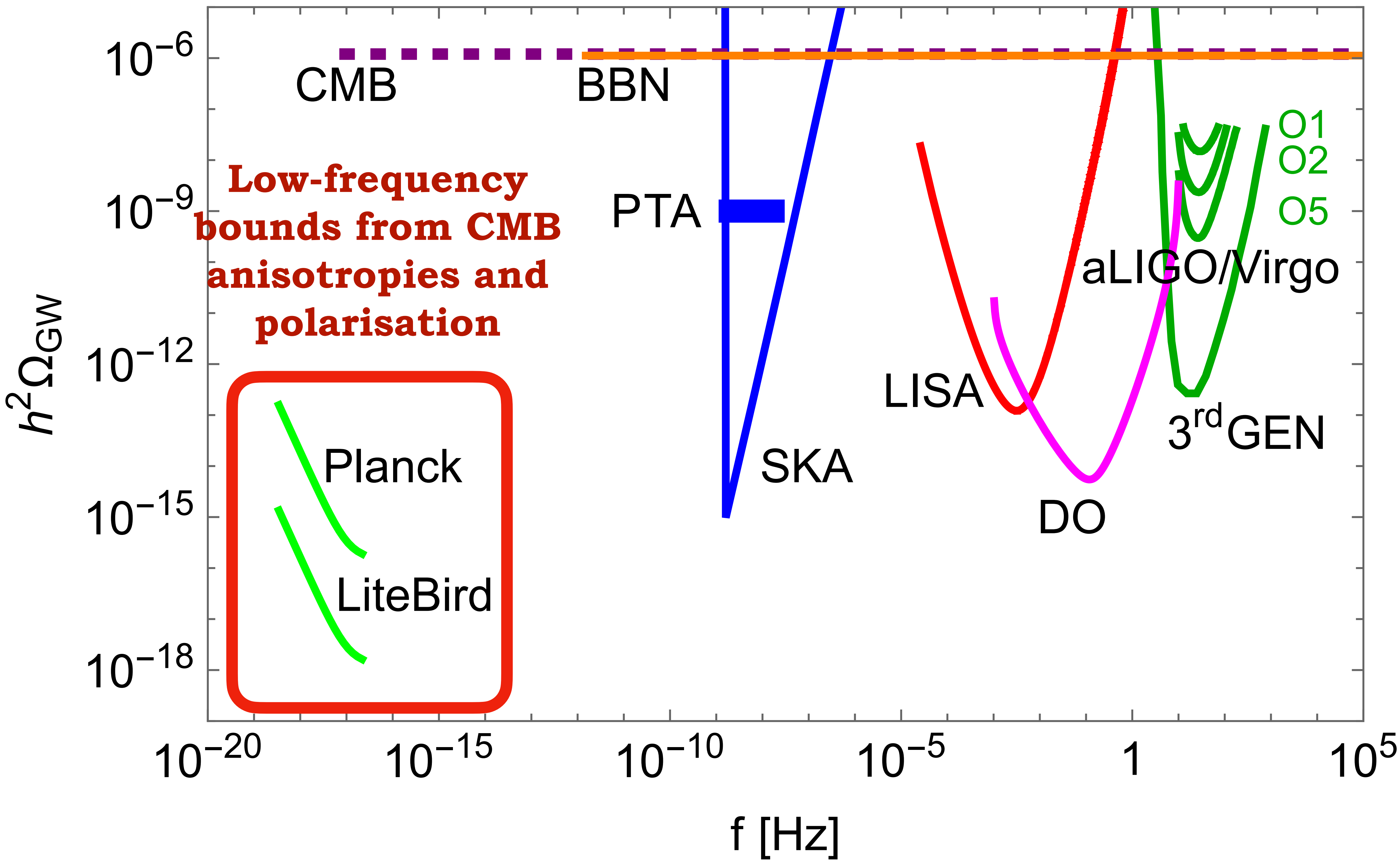

Cosmic microwave background

frequency range of detection: 10^{-18} Hz < f < 10^{-16} HZ

- temperature anisotropy:
  limit by Planck

$$\frac{\delta T}{T} = -\int_{t_{\rm dec}}^{t_0} \dot{h}_{ij}\, n^i n^j \, dt$$

$$P_h(k) = A_t(k_0)\,(k\,\eta_0)^{n_t} \qquad C_{\ell,T}^{\Theta\Theta} \simeq \frac{\sqrt{\pi}}{3} A_t(k_0)\, \frac{\ell(\ell+2)!}{(\ell-2)!}\, \frac{\Gamma\left[\frac{7-n_t}{2}\right]\Gamma\left[\ell+\frac{n_t}{2}\right]}{\Gamma\left[4-\frac{n_t}{2}\right]\Gamma\left[\ell+7-\frac{n_t}{2}\right]}$$

$$\propto \; \ell^{n_t-2} \qquad \text{for} \;\; 1 \ll \ell \lesssim 60$$

- polarisation: BB spectrum measured by BICEP2 and Planck generated at photon decoupling time, from Thomson scattering of electrons by a quadrupole temperature anisotropy in the photons

polarisation patterns

generated by primordial scalar and tensor perturbations

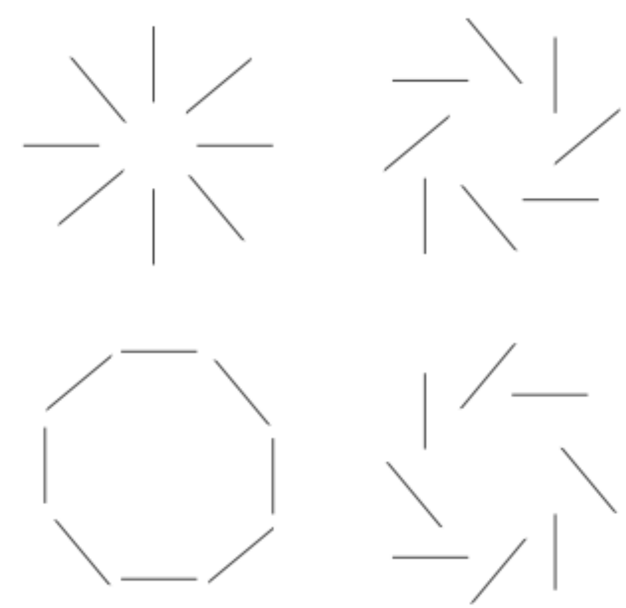

E mode B mode

generated only by primordial tensor perturbations or by foregrounds

Cosmic microwave background

Galloni et al: arXiv:2208.00188

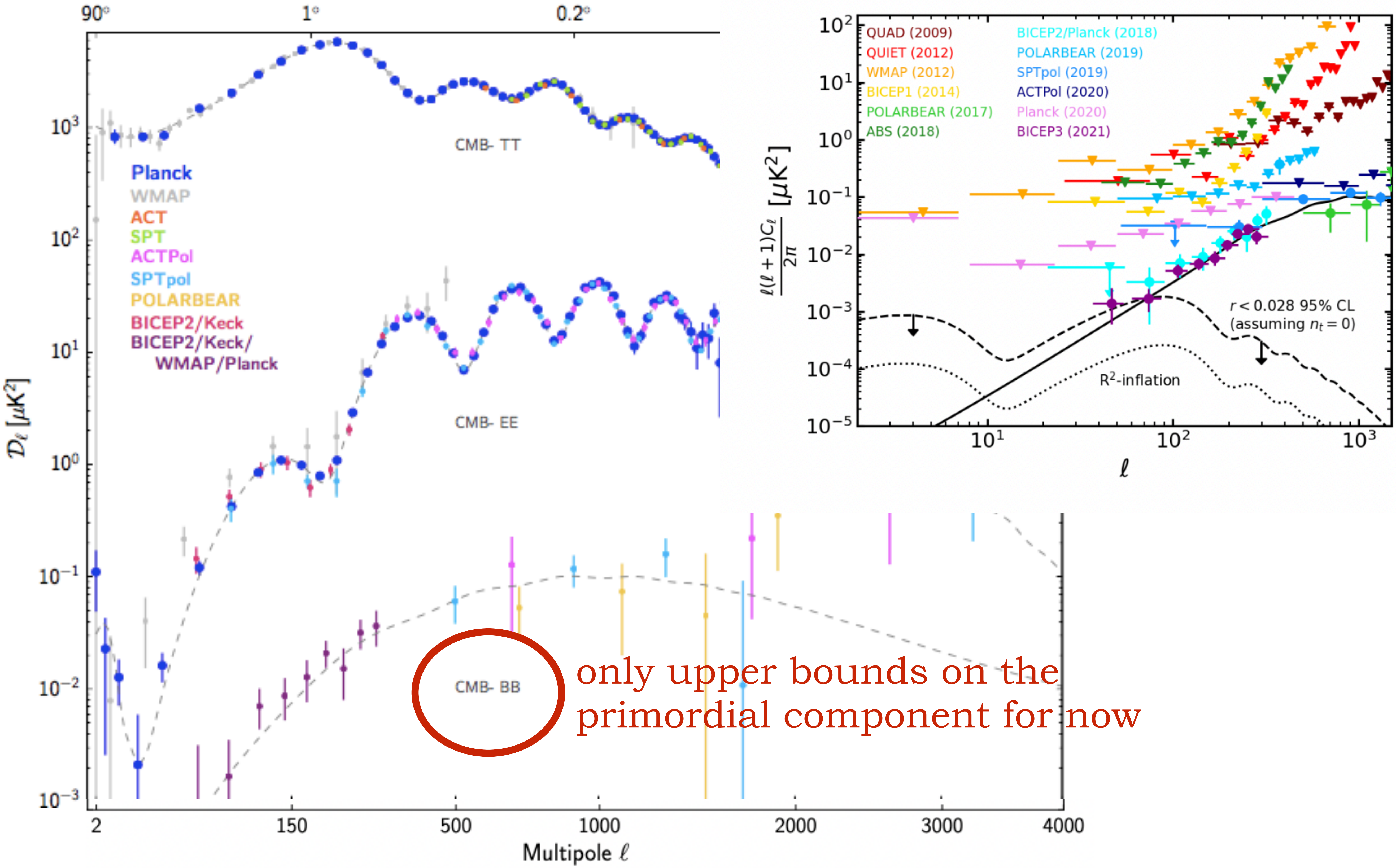

only upper bounds on the primordial component for now

Planck collaboration: arXiv:1807.06205

Cosmic microwave background

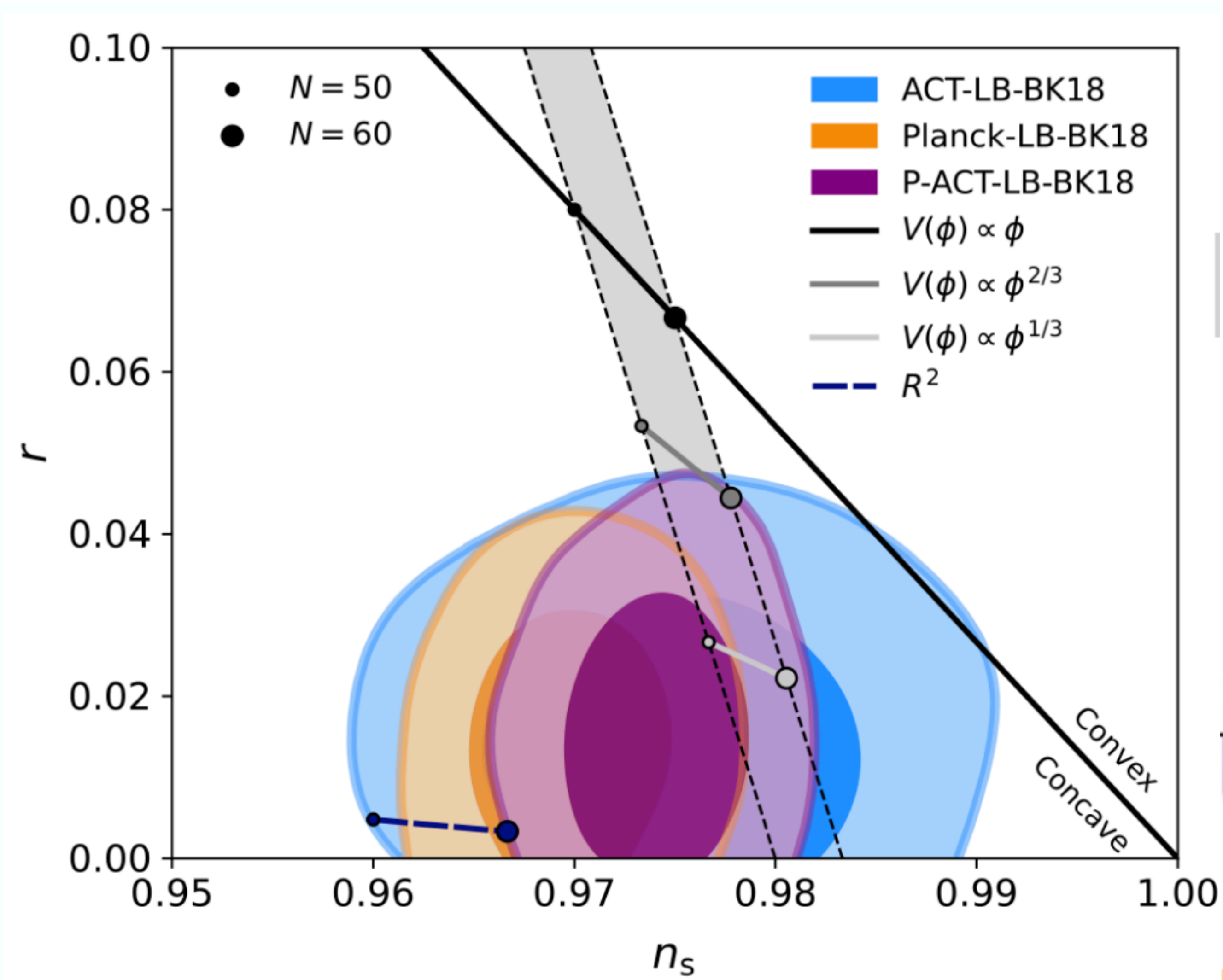

Calabrese et al, arXiv:2503.14454

This constraint is usually represented in the context of Inflation as a bound on the tensor-to-scalar ratio

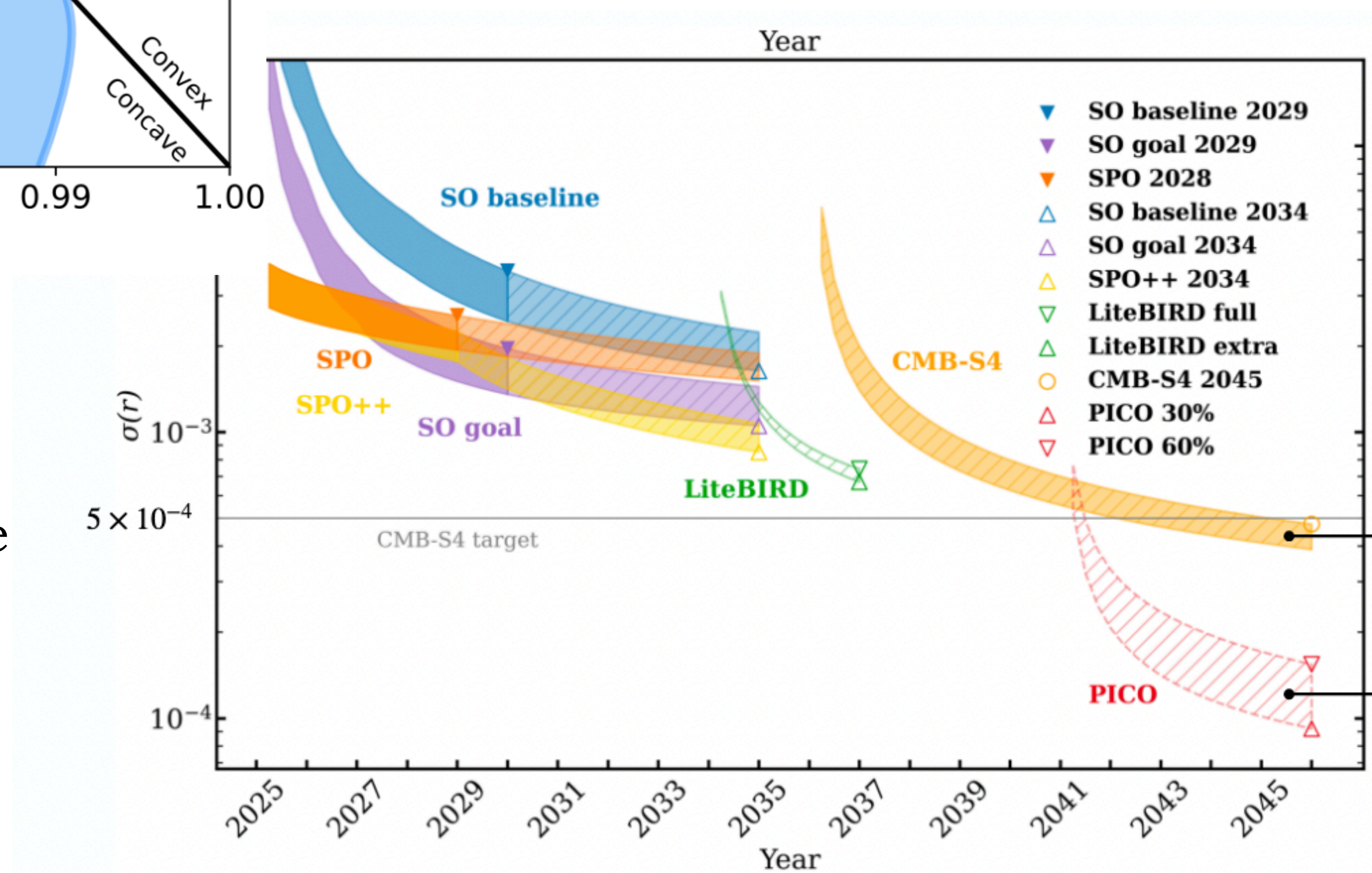

Projected sensitivity on the tensor-to-scalar ratio

What is/will be known about the SGWB

Present and future GW obsevatories: LVK

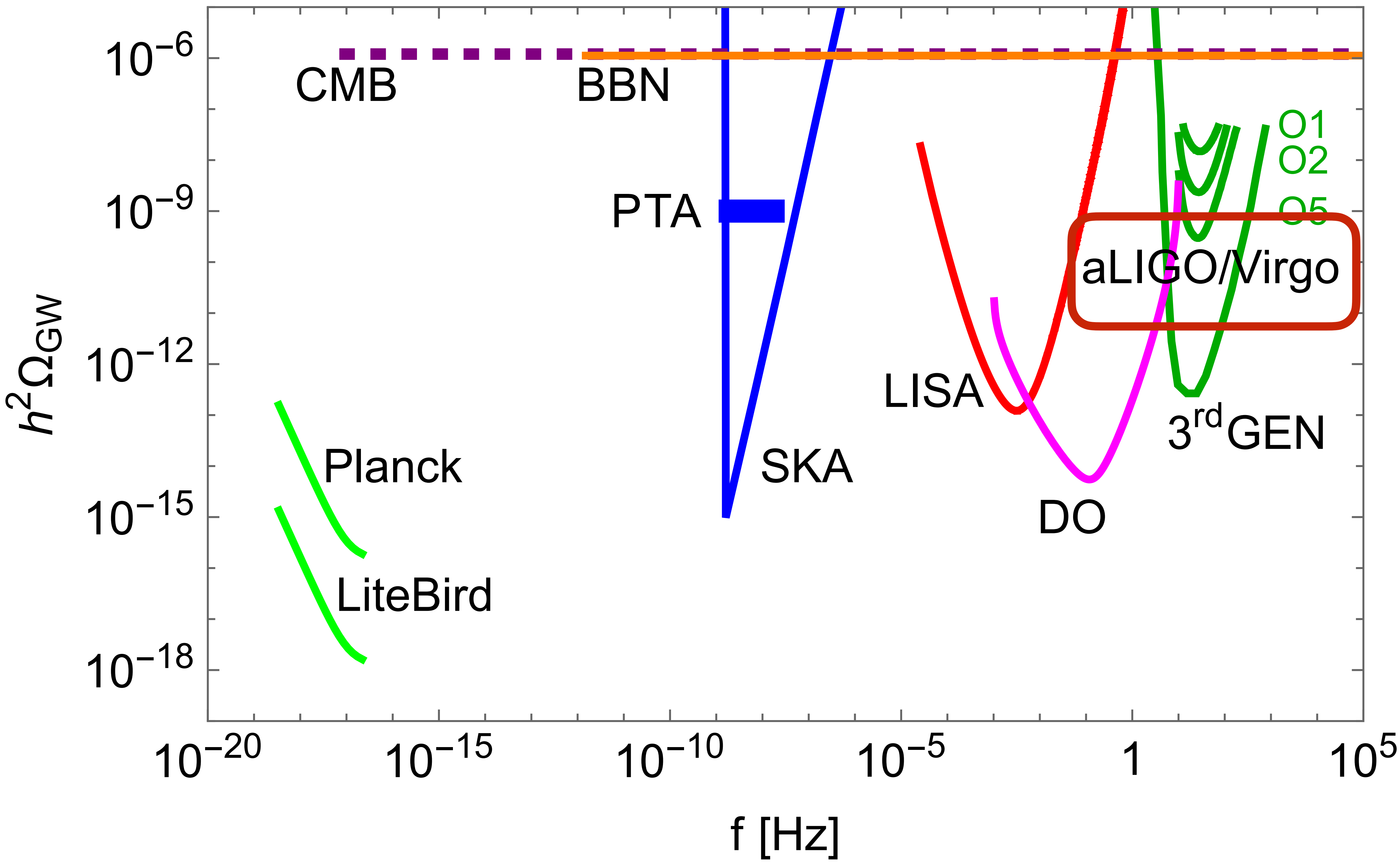

Earth-based interferometers

LIGO/Virgo (operating)

arm length L = 4 km

frequency range of detection:
10 Hz < f < 5kHZ

3rd generation ET, CE (future)

arm length L ~15-20 km

frequency range of detection:
1 Hz < f < 10^4 HZ

factor 20 improvement in sensitivity

DETECTION TARGETS:

- Black hole coalescing binaries of masses few to hundred solar masses (BHBs)
- Neutron Star and NS-BH binaries / SN explosions
- Stochastic GW background

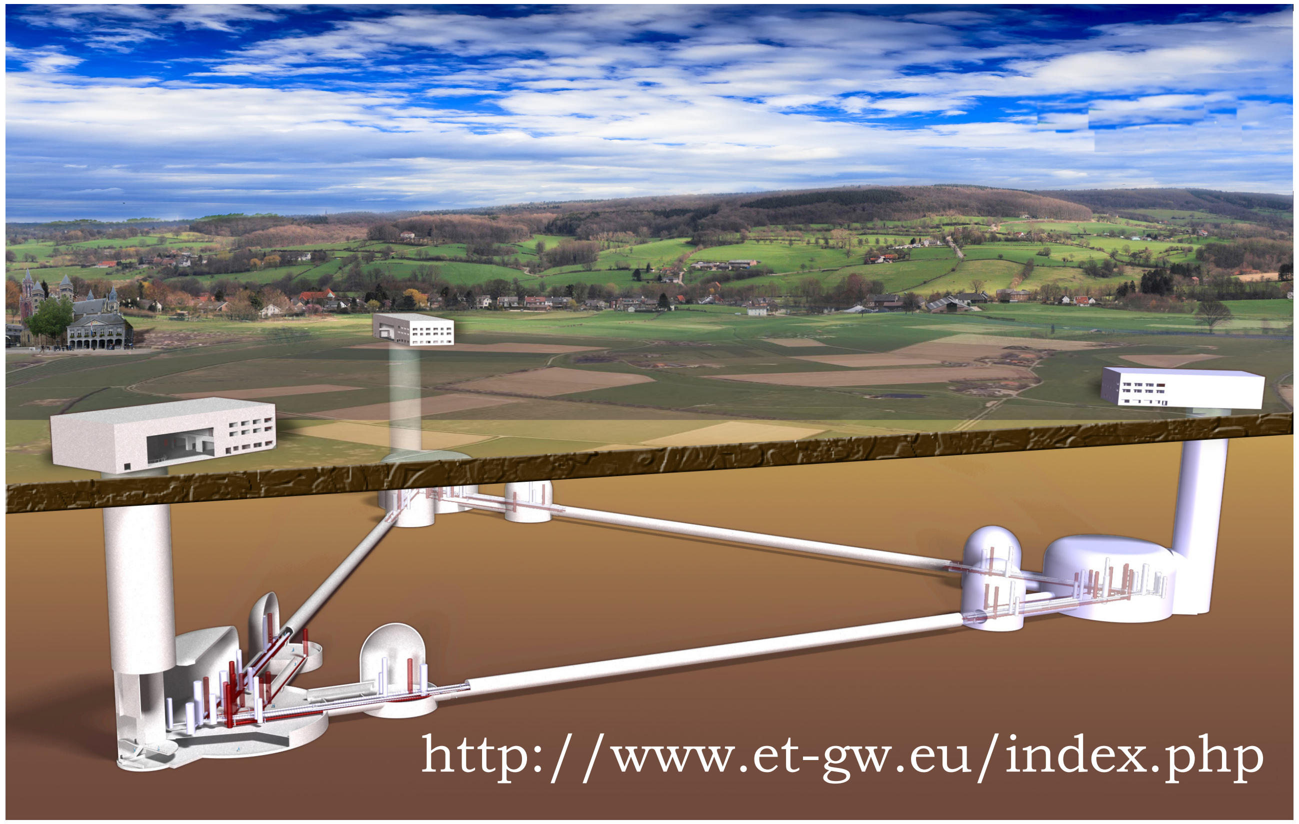

Earth-based interferometers

Candidate	$M(M_\odot)$	$\mathcal{M}(M_\odot)$	$m_1(M_\odot)$	$m_2(M_\odot)$	$\chi_{\rm eff}$	D_L(Gpc)	z	$M_f(M_\odot)$	χ_f	$\Delta\Omega$(deg^2)	SNR
GW191103_012549	$20.0^{+3.7}_{-1.8}$	$8.34^{+0.66}_{-0.57}$	$11.8^{+6.2}_{-2.2}$	$7.9^{+1.7}_{-2.4}$	$0.21^{+0.16}_{-0.10}$	$0.99^{+0.50}_{-0.47}$	$0.20^{+0.09}_{-0.09}$	$19.0^{+3.8}_{-1.7}$	$0.75^{+0.06}_{-0.05}$	2500	$8.9^{+0.3}_{-0.5}$
GW191105_143521	$18.5^{+2.1}_{-1.3}$	$7.82^{+0.61}_{-0.45}$	$10.7^{+3.7}_{-1.6}$	$7.7^{+1.4}_{-1.9}$	$-0.02^{+0.13}_{-0.09}$	$1.15^{+0.43}_{-0.48}$	$0.23^{+0.07}_{-0.09}$	$17.6^{+2.1}_{-1.2}$	$0.67^{+0.04}_{-0.05}$	640	$9.7^{+0.3}_{-0.5}$
GW191109_010717	112^{+20}_{-16}	$47.5^{+9.6}_{-7.5}$	65^{+11}_{-11}	47^{+15}_{-13}	$-0.29^{+0.42}_{-0.31}$	$1.29^{+1.13}_{-0.65}$	$0.25^{+0.18}_{-0.12}$	107^{+18}_{-15}	$0.61^{+0.18}_{-0.19}$	1600	$17.3^{+0.5}_{-0.5}$
GW191113_071753	$34.5^{+10.5}_{-9.8}$	$10.7^{+1.1}_{-1.0}$	29^{+12}_{-14}	$5.9^{+4.4}_{-1.3}$	$0.00^{+0.37}_{-0.29}$	$1.37^{+1.15}_{-0.62}$	$0.26^{+0.18}_{-0.11}$	34^{+11}_{-10}	$0.45^{+0.33}_{-0.11}$	3600	$7.9^{+0.5}_{-1.1}$
GW191126_115259	$20.7^{+3.4}_{-2.0}$	$8.65^{+0.95}_{-0.71}$	$12.1^{+5.5}_{-2.2}$	$8.3^{+1.9}_{-2.4}$	$0.21^{+0.15}_{-0.11}$	$1.62^{+0.74}_{-0.74}$	$0.30^{+0.12}_{-0.13}$	$19.6^{+3.5}_{-2.0}$	$0.75^{+0.06}_{-0.05}$	1400	$8.3^{+0.2}_{-0.5}$
GW191127_050227	80^{+39}_{-22}	$29.9^{+11.7}_{-9.1}$	53^{+47}_{-20}	24^{+17}_{-14}	$0.18^{+0.34}_{-0.36}$	$3.4^{+3.1}_{-1.9}$	$0.57^{+0.40}_{-0.29}$	76^{+39}_{-21}	$0.75^{+0.13}_{-0.29}$	980	$9.2^{+0.7}_{-0.6}$
GW191129_134029	$17.5^{+2.4}_{-1.2}$	$7.31^{+0.43}_{-0.28}$	$10.7^{+4.1}_{-2.1}$	$6.7^{+1.5}_{-1.7}$	$0.06^{+0.16}_{-0.08}$	$0.79^{+0.26}_{-0.33}$	$0.16^{+0.05}_{-0.06}$	$16.8^{+2.5}_{-1.2}$	$0.69^{+0.03}_{-0.05}$	850	$13.1^{+0.2}_{-0.3}$
GW191204_110529	$47.1^{+9.1}_{-7.8}$	$19.8^{+3.6}_{-3.2}$	$27.3^{+10.8}_{-5.9}$	$19.2^{+5.5}_{-6.0}$	$0.05^{+0.25}_{-0.26}$	$1.9^{+1.7}_{-1.1}$	$0.34^{+0.25}_{-0.18}$	$45.0^{+8.7}_{-7.5}$	$0.71^{+0.11}_{-0.11}$	3400	$8.9^{+0.4}_{-0.6}$
GW191204_171526	$20.19^{+1.64}_{-0.95}$	$8.56^{+0.41}_{-0.28}$	$11.7^{+3.3}_{-1.7}$	$8.4^{+1.3}_{-1.7}$	$0.16^{+0.08}_{-0.05}$	$0.64^{+0.20}_{-0.26}$	$0.13^{+0.04}_{-0.05}$	$19.18^{+1.71}_{-0.93}$	$0.73^{+0.04}_{-0.03}$	310	$17.4^{+0.2}_{-0.3}$
GW191215_223052	$43.3^{+5.3}_{-4.3}$	$18.4^{+2.2}_{-1.7}$	$24.9^{+7.1}_{-4.1}$	$18.1^{+3.8}_{-4.1}$	$-0.04^{+0.17}_{-0.21}$	$1.93^{+0.89}_{-0.86}$	$0.35^{+0.13}_{-0.14}$	$41.4^{+5.1}_{-4.1}$	$0.68^{+0.07}_{-0.07}$	530	$11.2^{+0.3}_{-0.4}$
GW191216_213338	$19.80^{+2.70}_{-0.93}$	$8.33^{+0.22}_{-0.19}$	$12.1^{+4.6}_{-2.2}$	$7.7^{+1.6}_{-1.9}$	$0.11^{+0.13}_{-0.06}$	$0.34^{+0.12}_{-0.13}$	$0.07^{+0.02}_{-0.03}$	$18.87^{+2.81}_{-0.93}$	$0.70^{+0.03}_{-0.04}$	910	$18.6^{+0.2}_{-0.2}$
GW191219_163120	$32.3^{+2.2}_{-2.7}$	$4.31^{+0.12}_{-0.17}$	$31.1^{+2.2}_{-2.8}$	$1.17^{+0.07}_{-0.06}$	$0.00^{+0.07}_{-0.09}$	$0.55^{+0.24}_{-0.16}$	$0.11^{+0.05}_{-0.03}$	$32.2^{+2.2}_{-2.7}$	$0.14^{+0.06}_{-0.06}$	1500	$9.1^{+0.5}_{-0.8}$
GW191222_033537	79^{+16}_{-11}	$33.8^{+7.1}_{-5.0}$	$45.1^{+10.9}_{-8.0}$	$34.7^{+9.3}_{-10.5}$	$-0.04^{+0.20}_{-0.25}$	$3.0^{+1.7}_{-1.7}$	$0.51^{+0.23}_{-0.26}$	$75.5^{+15.3}_{-9.9}$	$0.67^{+0.08}_{-0.11}$	2000	$12.5^{+0.2}_{-0.3}$
GW191230_180458	86^{+19}_{-12}	$36.5^{+8.2}_{-5.6}$	$49.4^{+14.0}_{-9.6}$	37^{+11}_{-12}	$-0.05^{+0.26}_{-0.31}$	$4.3^{+2.1}_{-1.9}$	$0.69^{+0.26}_{-0.27}$	82^{+17}_{-11}	$0.68^{+0.11}_{-0.13}$	1100	$10.4^{+0.3}_{-0.4}$
GW200105_162426	$11.0^{+1.5}_{-1.4}$	$3.42^{+0.08}_{-0.08}$	$9.1^{+1.7}_{-1.7}$	$1.91^{+0.33}_{-0.24}$							
GW200112_155838	$63.9^{+5.7}_{-4.6}$	$27.4^{+2.6}_{-2.1}$	$35.6^{+6.7}_{-4.5}$	$28.3^{+4.4}_{-5.9}$							
GW200115_042309	$7.4^{+1.7}_{-1.7}$	$2.43^{+0.05}_{-0.07}$	$5.9^{+2.0}_{-2.5}$	$1.44^{+0.85}_{-0.28}$							
GW200128_022011	75^{+17}_{-12}	$32.0^{+7.5}_{-5.5}$	$42.2^{+11.6}_{-8.1}$	$32.6^{+9.5}_{-9.2}$							
GW200129_065458	$63.3^{+4.5}_{-3.4}$	$27.2^{+2.1}_{-2.3}$	$34.5^{+9.9}_{-3.1}$	$29.0^{+3.3}_{-9.3}$							
GW200202_154313	$17.58^{+1.78}_{-0.67}$	$7.49^{+0.24}_{-0.20}$	$10.1^{+3.5}_{-1.4}$	$7.3^{+1.1}_{-1.7}$							
GW200208_130117	$65.3^{+8.1}_{-6.8}$	$27.7^{+3.7}_{-3.1}$	$37.7^{+9.3}_{-6.2}$	$27.4^{+6.3}_{-7.3}$							
GW200208_222617	63^{+100}_{-26}	$19.8^{+10.5}_{-5.2}$	51^{+103}_{-30}	$12.3^{+9.2}_{-5.5}$							
GW200209_085452	$62.6^{+13.9}_{-9.4}$	$26.7^{+6.0}_{-4.2}$	$35.6^{+10.5}_{-6.8}$	$27.1^{+7.8}_{-7.8}$							
GW200210_092254	$27.0^{+7.1}_{-4.3}$	$6.56^{+0.38}_{-0.40}$	$24.1^{+7.5}_{-4.6}$	$2.83^{+0.47}_{-0.42}$							
GW200216_220804	81^{+20}_{-14}	$32.9^{+9.3}_{-8.5}$	51^{+22}_{-13}	30^{+14}_{-16}							
GW200219_094415	$65.0^{+12.6}_{-8.2}$	$27.6^{+5.6}_{-3.8}$	$37.5^{+10.1}_{-6.9}$	$27.9^{+7.4}_{-8.4}$							
GW200220_061928	148^{+55}_{-33}	62^{+23}_{-15}	87^{+40}_{-23}	61^{+26}_{-25}							
GW200220_124850	67^{+17}_{-12}	$28.2^{+7.3}_{-5.1}$	$38.9^{+14.1}_{-8.6}$	$27.9^{+9.2}_{-9.0}$							
GW200224_222234	$72.3^{+7.2}_{-5.3}$	$31.1^{+3.3}_{-2.7}$	$40.0^{+6.7}_{-4.5}$	$32.7^{+4.8}_{-7.2}$							
GW200225_060421	$33.5^{+3.6}_{-3.0}$	$14.2^{+1.5}_{-1.4}$	$19.3^{+5.0}_{-3.0}$	$14.0^{+2.8}_{-3.5}$							
GW200302_015811	$57.8^{+9.6}_{-6.9}$	$23.4^{+4.7}_{-3.0}$	$37.8^{+8.7}_{-8.5}$	$20.0^{+8.1}_{-5.7}$							
GW200306_093714	$43.9^{+11.8}_{-7.5}$	$17.5^{+3.5}_{-3.0}$	$28.3^{+17.1}_{-7.7}$	$14.8^{+6.5}_{-6.4}$							
GW200308_173609*	92^{+169}_{-48}	34^{+44}_{-18}	60^{+166}_{-29}	24^{+36}_{-13}							
GW200311_115853	$61.9^{+5.3}_{-4.2}$	$26.6^{+2.4}_{-2.0}$	$34.2^{+6.4}_{-3.8}$	$27.7^{+4.1}_{-5.9}$							
GW200316_215756	$21.2^{+7.2}_{-2.0}$	$8.75^{+0.62}_{-0.55}$	$13.1^{+10.2}_{-2.9}$	$7.8^{+2.0}_{-2.9}$							
GW200322_091133*	50^{+132}_{-22}	$15.0^{+29.5}_{-4.0}$	38^{+130}_{-22}	$11.3^{+24.3}_{-6.0}$							

Individually resolved BHBs, NSBs, NS-BH

Last catalogue GWTC-3:

90 binary mergers detected, including NS-BH and NS-NS mergers

LVK Collaboration: arXiv:2111.03606

Earth-based interferometers

Stochastic GW background: for now, only upper bounds

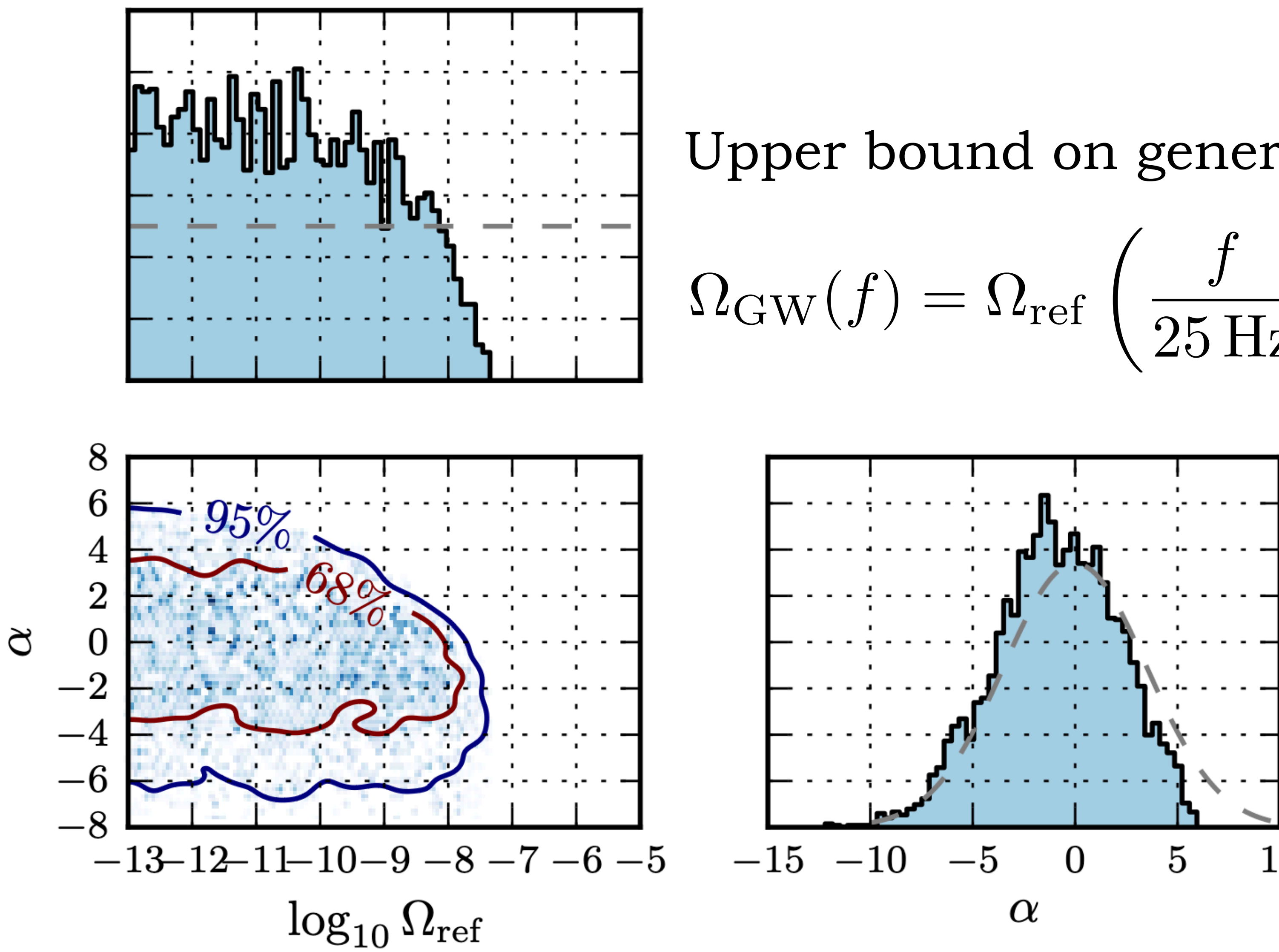

Upper bound on generic

$$\Omega_{\rm GW}(f) = \Omega_{\rm ref}\left(\frac{f}{25\,\mathrm{Hz}}\right)^{\alpha}$$

Most probably no cosmological SGWB detection by LVK, masked by astrophysical foreground detection expected for ~2030

SGWB from BHBs and NSBs

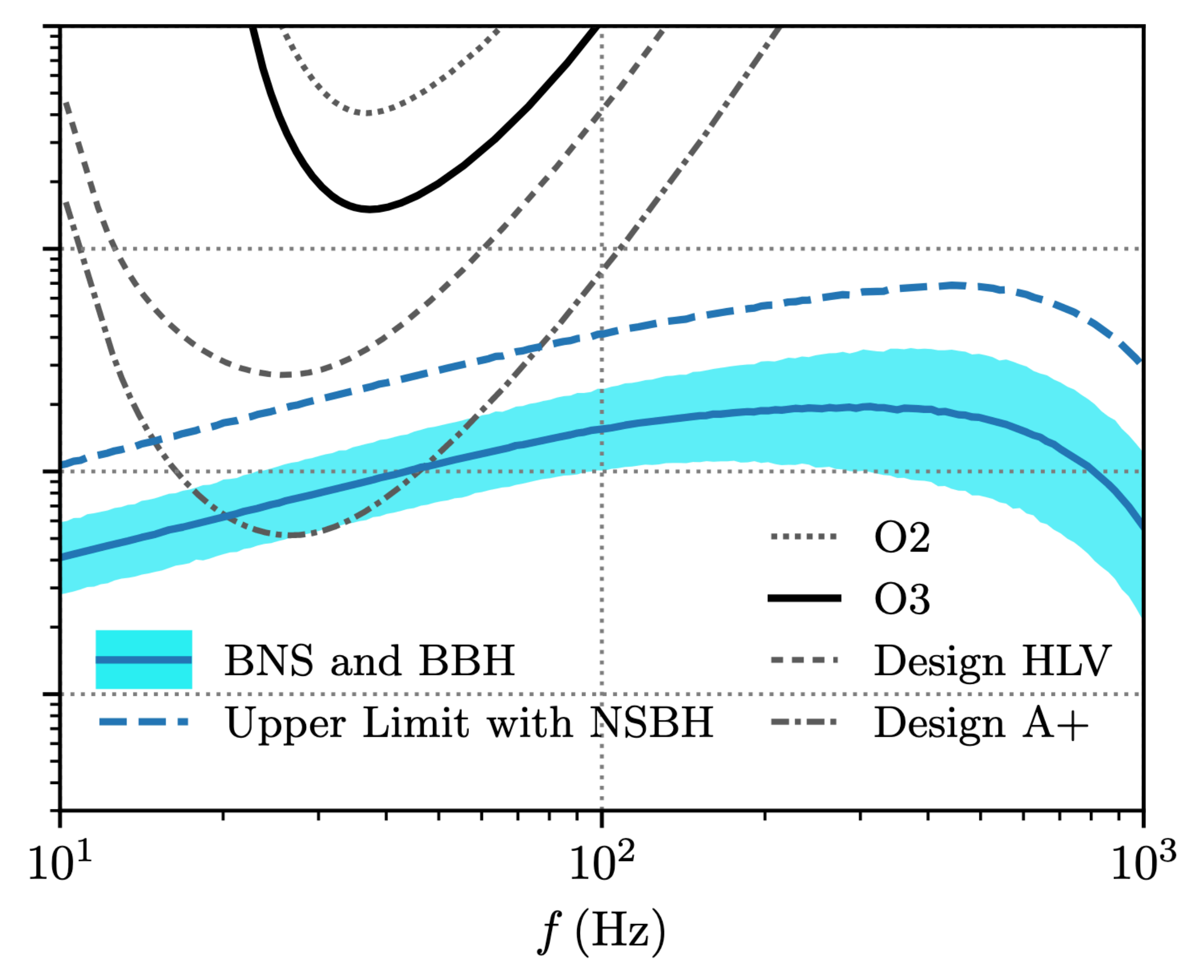

Detection via cross-correlation of signals from different detectors

LVK Collaborations, arXiv:2101.12130

What is/will be known about the SGWB

Present and future GW observatories: LISA

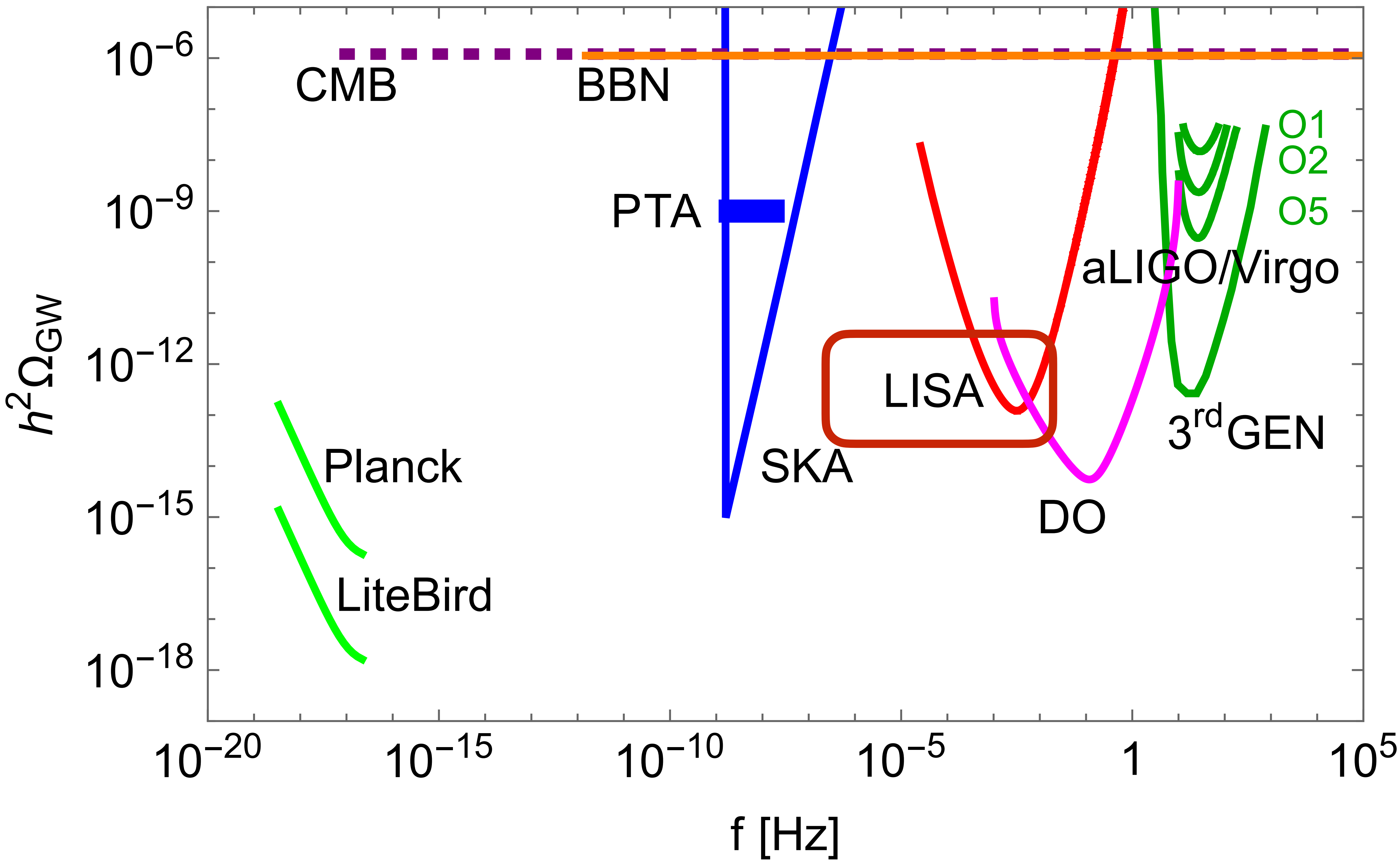

Space-based interferometers: LISA

LISA: Laser Interferometer Space Antenna

- no seismic noise
- much longer arms than on Earth

frequency range of detection:

$$10^{-4}\,\mathrm{Hz} < f < 1\,\mathrm{Hz}$$

- Launch in ~2035
- two masses in free fall per spacecraft
- 2.5 million km arms
- picometer displacement of masses

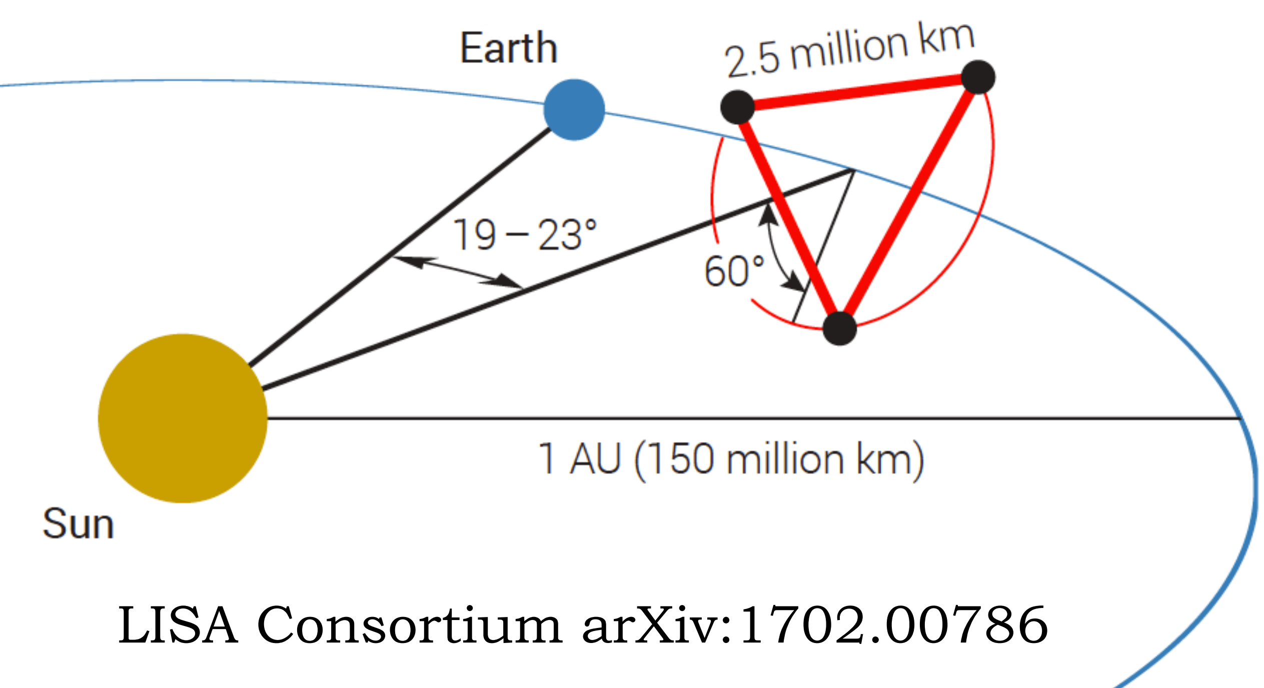

LISA Consortium arXiv:1702.00786

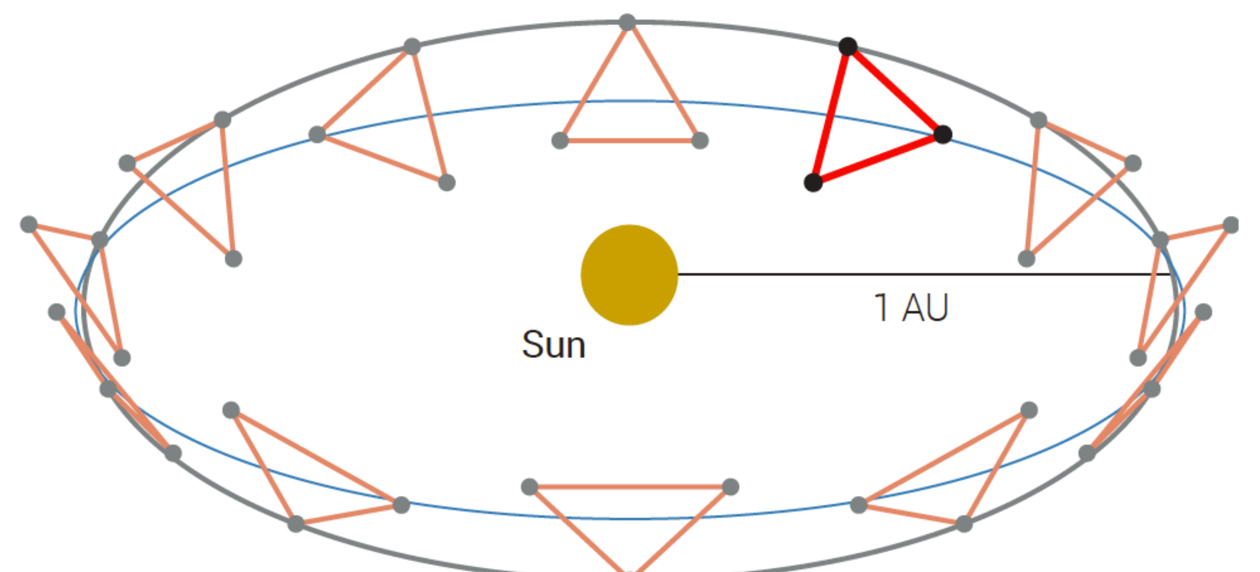

Space-based interferometers: LISA

DETECTION TARGETS:

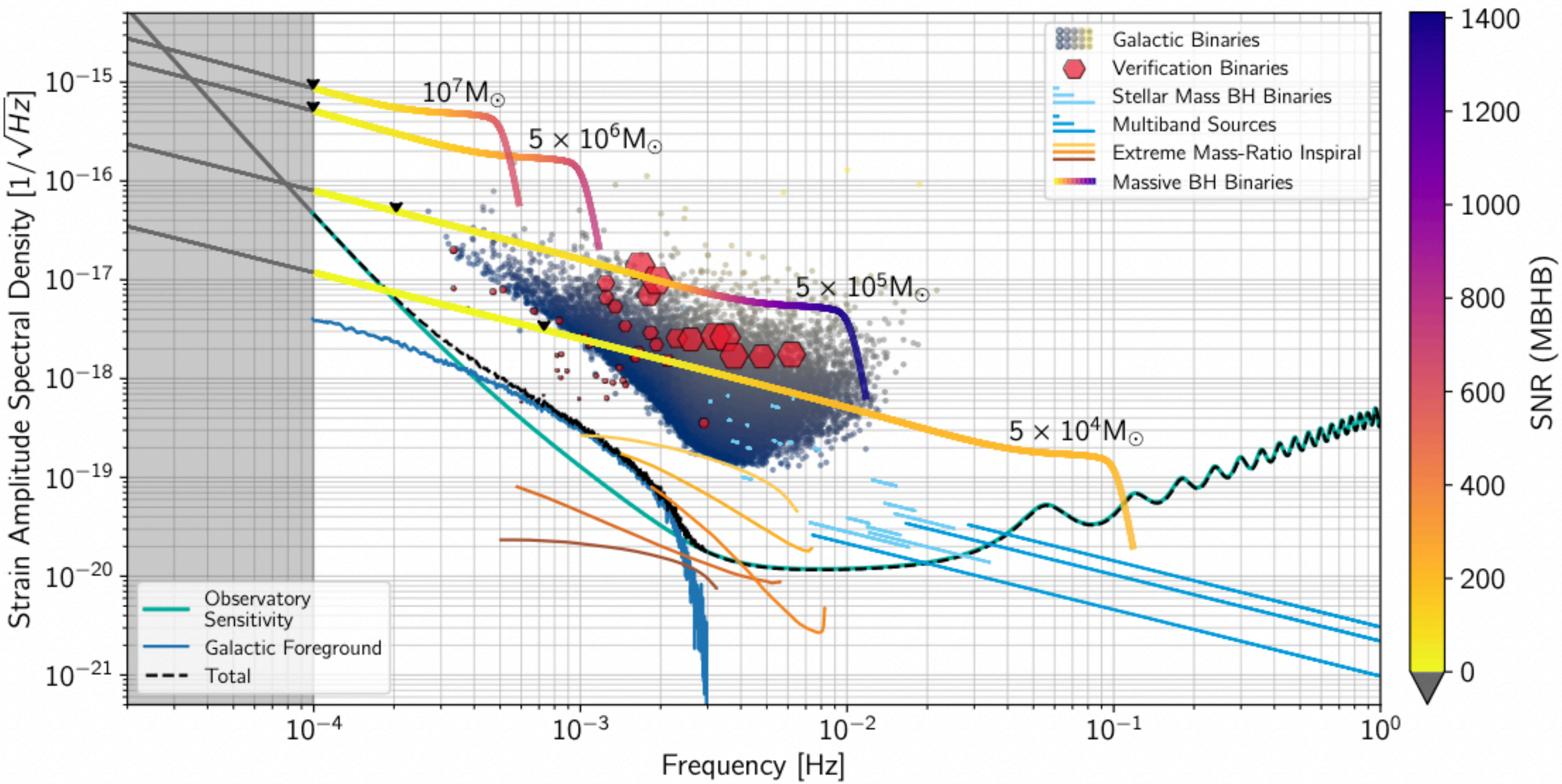

M. Colpi et al, arXiv:2402.07571 - LISA Red Book

Space-based interferometers: LISA

Stochastic GW background

- Confusion noise from the binaries in the Galaxy (mainly WD binaries)
- Confusion noise from extra-galactic binaries (WD binaries and BHBs)
- Candidates from the early universe, in particular at the EW scale

Detecting a SGWB with LISA is challenging: no cross-correlation, need to assume knowledge of the noise (possibility of null channels)

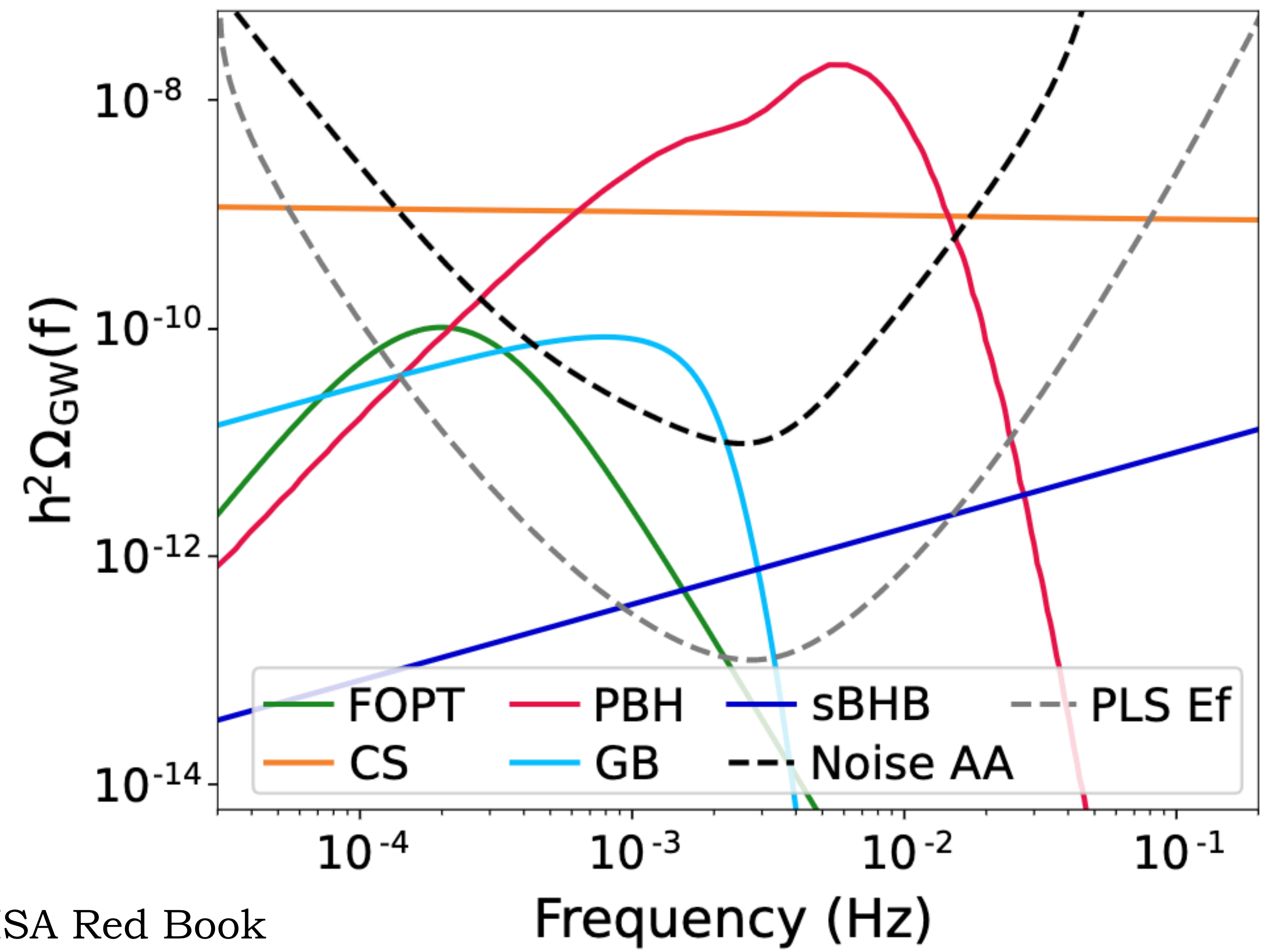

M. Colpi et al, arXiv:2402.07571 - LISA Red Book

What is/will be known about the SGWB

Present and future GW observatories: PTA

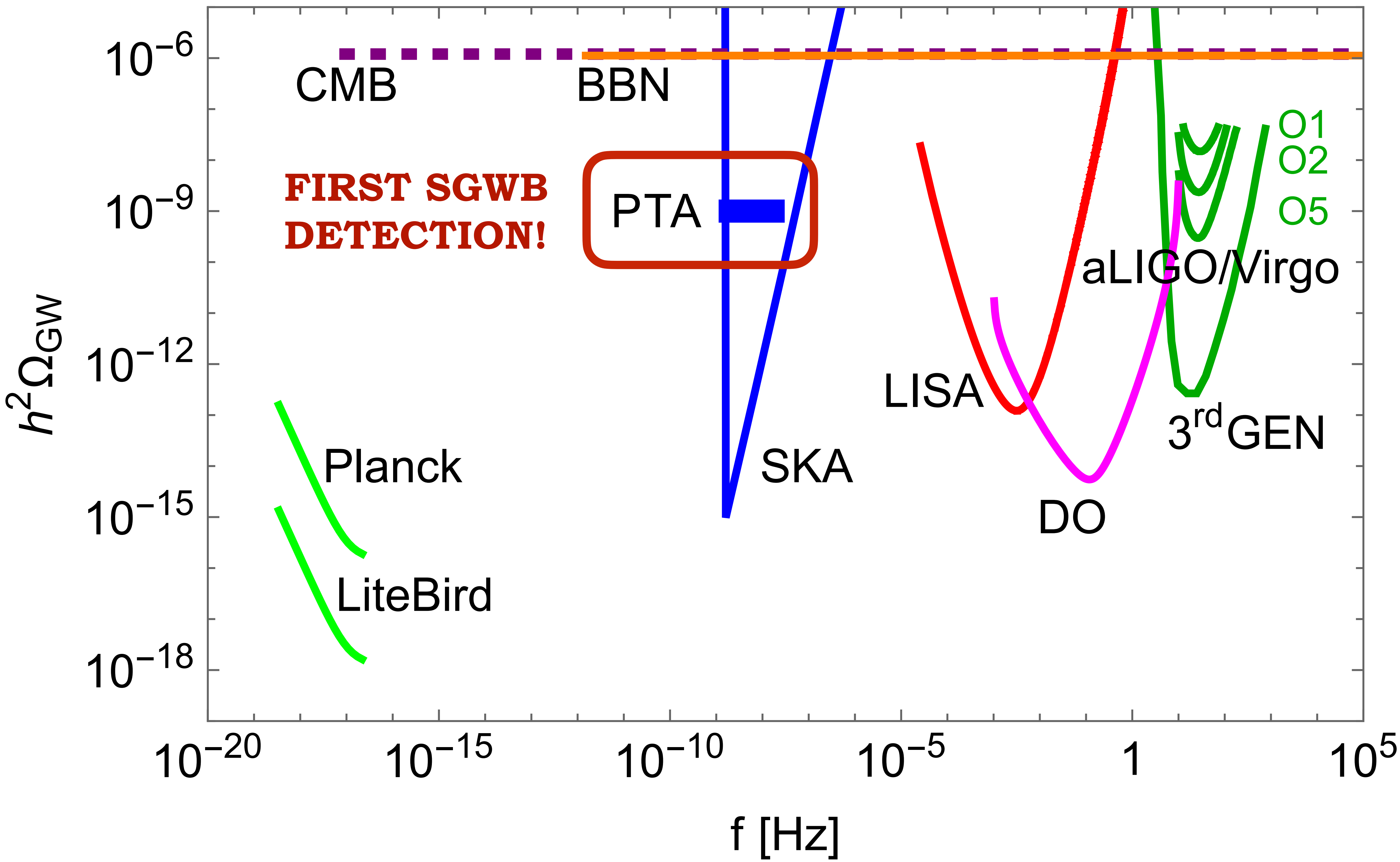

Pulsar timing arrays

CPTA, EPTA, NANOGrav, PPTA -> IPTA

frequency range of detection: 10^{-9} Hz < f < 10^{-7} HZ

- rotating, magnetised neutron stars emitting periodic radio-frequency EM pulses -> can be used as clocks in the sky

- the radio pulses are emitted at very regular time intervals, but their arrival times can be altered by a GW passing between the pulsar and the Earth

- First a timing model of the pulsar is constructed, which is then compared to observations to infer the *timing residuals* where the GW effect is looked for

DETECTION TARGETS:

Individual emission and stochastic background from inspiralling Super Massive Black Hole Binaries (SMBHBs) with masses ~10^9 $M_\odot$ at the centre of galaxies

Pulsar timing arrays

Principle of the measurement: gravitational redshift caused by gravitational waves emitted by far-away sources and travelling through spacetime between the pulsars and the Earth

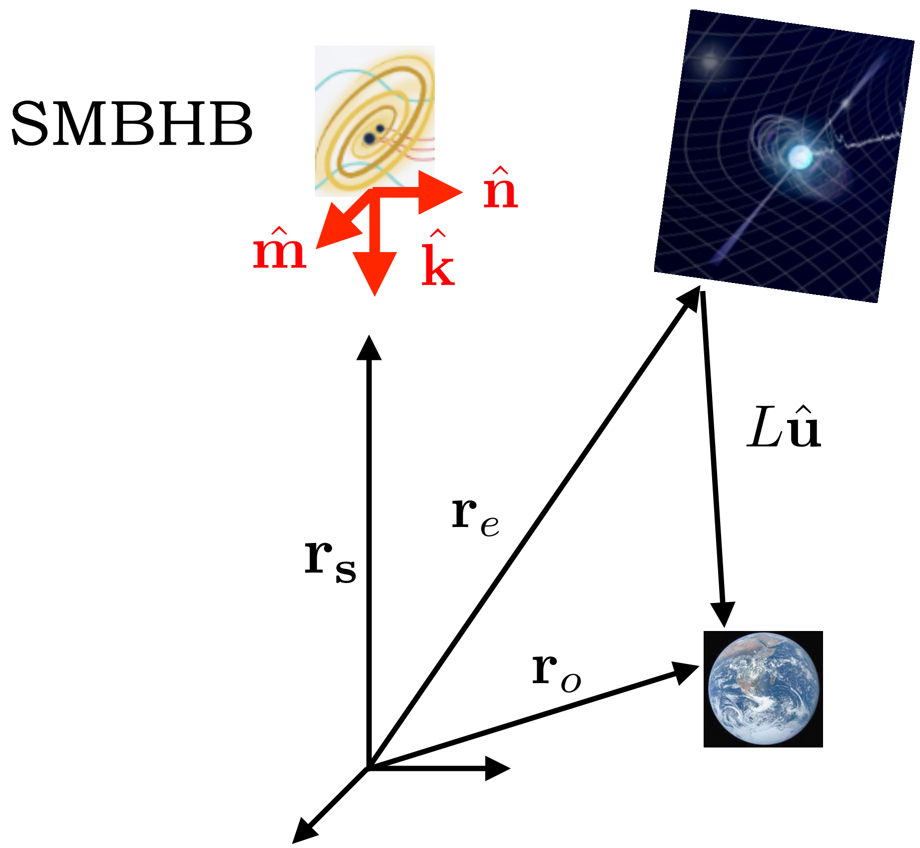

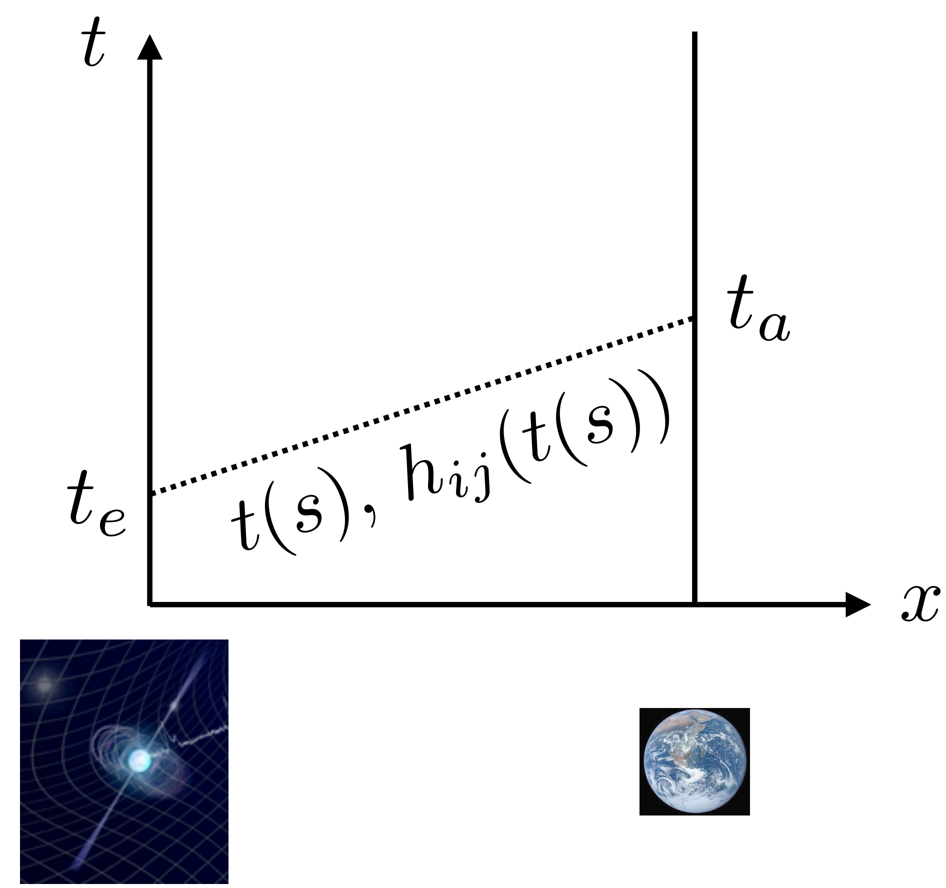

Photon from pulsar:

$$dt = \pm\sqrt{(\delta_{ij} + h_{ij})\mathrm{d}x^i\mathrm{d}x^j} \qquad t_a - t_e = L + \frac{1}{2}\hat{u}^i\hat{u}^j\int_0^L \mathrm{d}s\, h_{ij}(t_e + s, \mathbf{r_e} + s\hat{\mathbf{u}})$$

Effect of the metric perturbation on a single beam:
not measurable unless one knows the reference quantities

Pulsar timing arrays

Principle of the measurement: compare with the next pulse

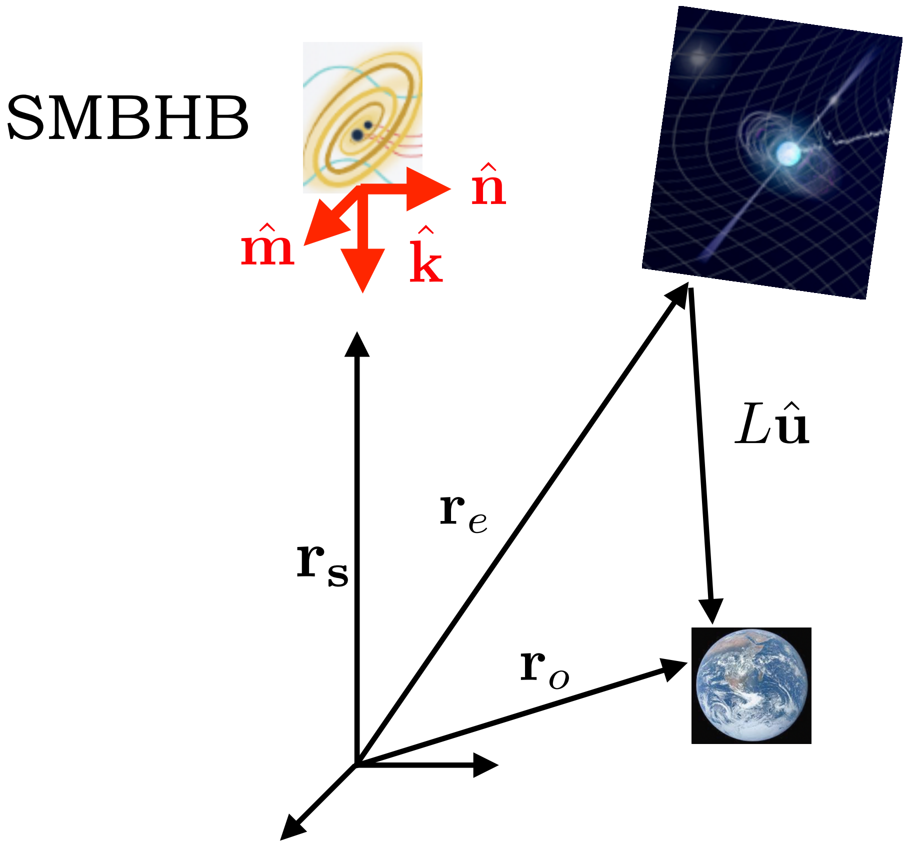

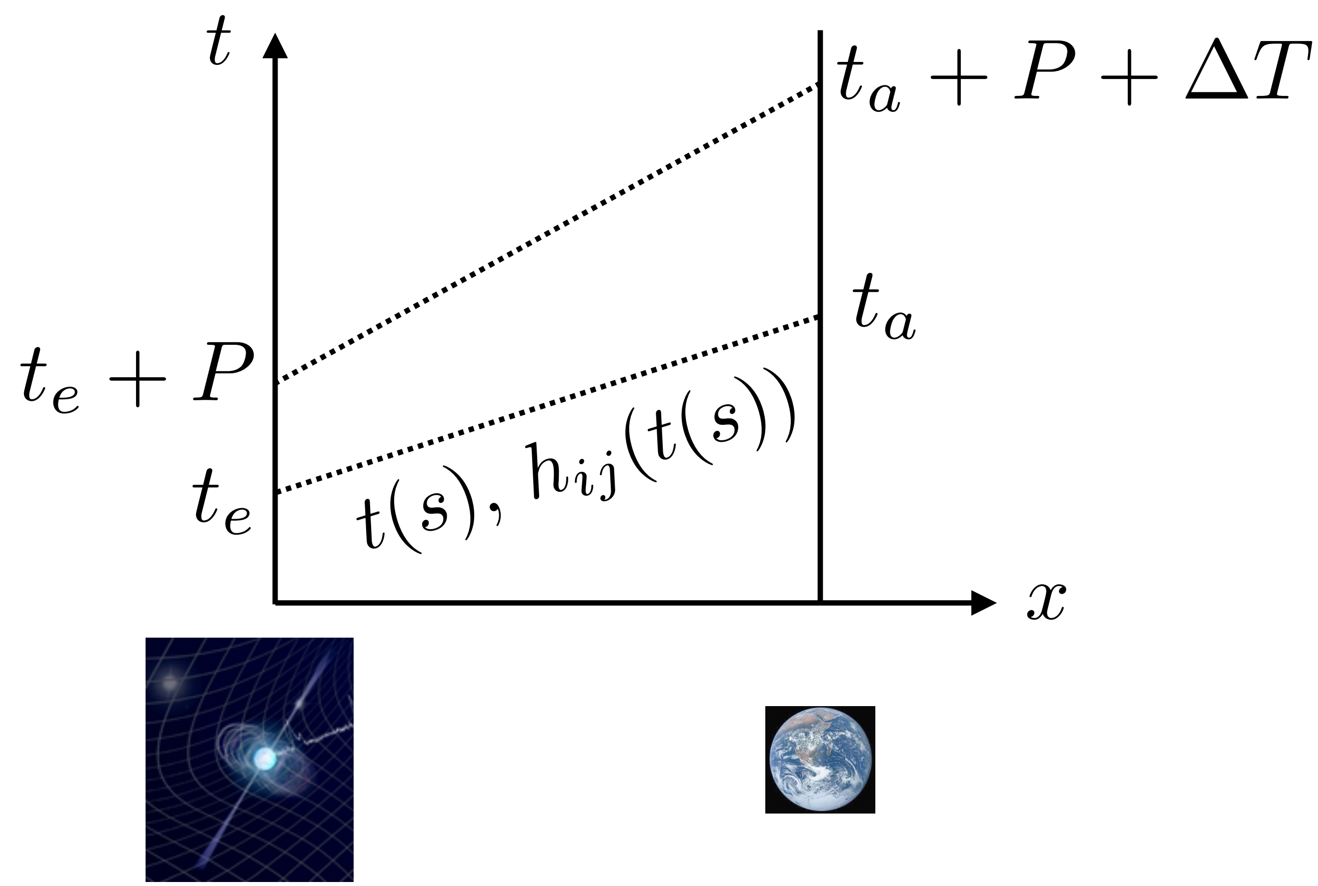

$$\Delta T = \frac{1}{2}\hat{u}^i\hat{u}^j \int_0^L \mathrm{d}s \left[h_{ij}(t_e + P + s, \mathbf{r_e} + s\hat{\mathbf{u}}) - h_{ij}(t_e + s, \mathbf{r_e} + s\hat{\mathbf{u}})\right]$$

This effect is present only because the gravitational wave is time-dependent

"Gravitational Waves Vol 2",
M. Maggiore, Oxford University Press 2018

S. Taylor, arXiv:2105.13270

Pulsar timing arrays

Principle of the measurement: compare with the next pulse

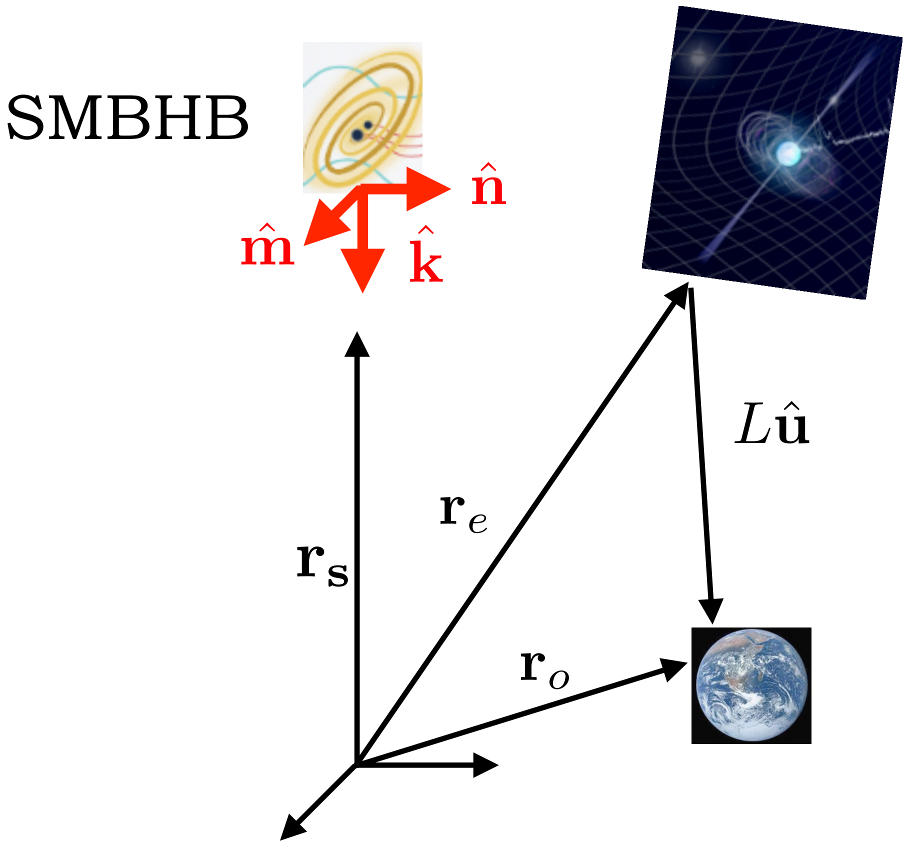

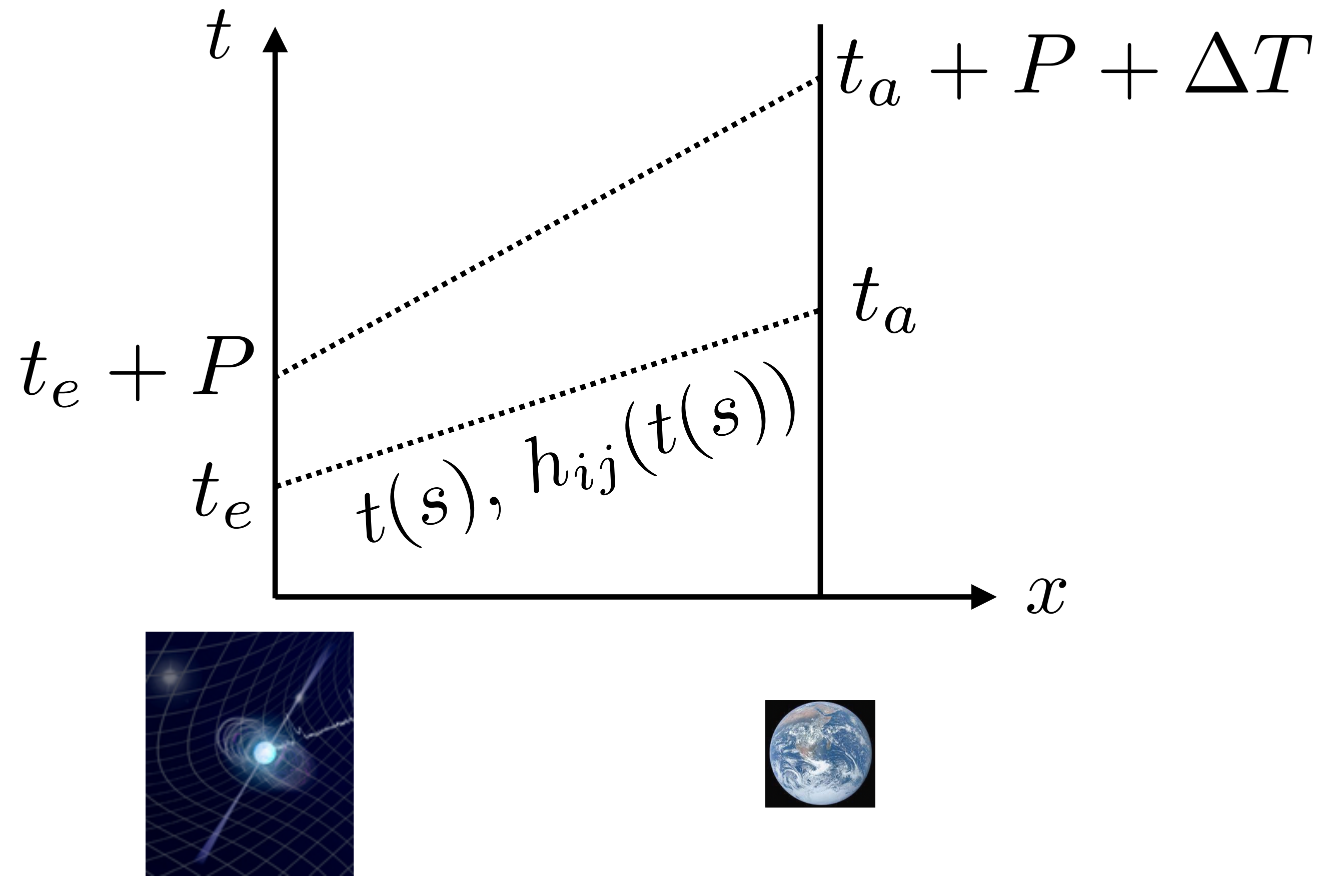

$$\Delta T = \frac{1}{2}\frac{\hat{u}^i\hat{u}^j}{1-\hat{\mathbf{k}}\cdot\hat{\mathbf{u}}}\int_{t_e-\hat{\mathbf{k}}\cdot\mathbf{r_e}}^{t_e+L-\hat{\mathbf{k}}\cdot\mathbf{r_e}-L\hat{\mathbf{k}}\cdot\mathbf{u}} \mathrm{d}X\,[h_{ij}(X+P)-h_{ij}(X)]$$

Wave propagating in k direction: $h_{ij}(X)$ with $X = t_e + s - \hat{\mathbf{k}}\cdot\mathbf{r_e} - s\,\hat{\mathbf{k}}\cdot\hat{\mathbf{u}}$